



Low frequency instability in laboratory-scale hybrid rocket motors

Kyung-Su Park¹, Changjin Lee*

Department of Aerospace Engineering, Konkuk University, Seoul 143-701, Republic of Korea

ARTICLE INFO

Article history:

Received 9 July 2014

Received in revised form 12 January 2015

Accepted 17 January 2015

Available online 22 January 2015

Keywords:

Hybrid rocket motor

Low frequency instability

Combustion experiment

ABSTRACT

Hybrid rocket combustion frequently displays a sudden amplification of combustion pressures leading into low frequency instability (LFI) with peak frequency of 10–20 Hz. A series of experimental tests was designed to examine the triggering mechanism of LFI, which occurred at a certain combustion condition. To this end, a couple of parameters was selected and the sensitivity of each parameter to instability was evaluated including volume ratios between main and post chambers, oxidizer mass flow rates, and solid fuel types. The results showed that the initiation of LFI was related to the flow modifications caused by vortex shedding and volume ratios between main and post chambers. Once LFI was initiated at a certain chamber configuration, the variation of oxidizer mass flow rates and the use of different solid fuel did not alter the triggering mechanism of LFI. Additional attention was focused to understand the critical role of vortex shedding on the initiation of LFI in the post chamber. The results confirmed that pressure oscillations by the thermal lag of solid fuel could be suddenly amplified, which leads to LFI in the case of resonating with unknown sources of pressure oscillations associated with vortex shedding in the post chamber. However, the details of triggering mechanism and the coupling of vortex shedding with additional pressure perturbations still remain unresolved.

© 2015 Elsevier Masson SAS. All rights reserved.

1. Introduction

Combustion in hybrid rocket motors is a relatively complex procedure to understand because of complicated coupling with fuel regressions, convective heat transfer, and diffusional flame in the turbulent boundary layer of chemically reacting flow. Combustion in hybrid rocket motors displays usually stable characteristics compared to other conventional chemical rockets such as solid and liquid rockets. Nonetheless, typical oscillations with a peak frequency much lower than acoustic modes were frequently found. Even though the causes of the instability are not clearly understood yet, it is suspected that a coupling of various types of pressure oscillation from different sources is the primary cause of low frequency instability (LFI).

A summary of physical explanation of LFI mechanism in hybrid rocket motors was addressed in Ref. [4]. This includes the response of low impedance oxidizer feeding system, combustion response to externally imposed pressure oscillations, periodic accumulation and break-off of melted layers from the fuel surface, and the time lag of vaporization and the combustion of liquid droplets. Each mechanism seemed to be responsible for generating a typical fre-

quency range of oscillation based on the characteristics of primary responses. For example, low frequency oscillations (≤ 100 Hz) are the results of coupling of oxidizer feeding system with pressure oscillations due to time lag responses of solid fuel. However, the unbounded high frequency pressure oscillations (> 1000 Hz) usually observed in solid and liquid propulsion systems were seldom found in hybrid rocket combustion. Instead, low frequency oscillations less than 50 Hz were dominantly observed.

Many studies have been investigated on the initiation mechanisms of LFI. Jenkins et al. [4] studied low frequency oscillations with a peak frequency of about 10 Hz using 1-D theoretical model. In particular, they investigated a filling time of oxidizer flux in the motor as the primary causes of low frequency oscillations by using a modified characteristic length (L^*). Lee [7] theoretically suggested that a transient behavior of thermal response of the solid fuel to quasi-steady heat input from the gas phase could be the initiation mechanism of low frequency oscillations. This is generally known as thermal lag oscillations, mainly observed in solid rocket motors due to the different thermal response of gas and solid phases to heat transfer from gas phase.

Karabeyoglu et al. [5] revealed that LFI was the result of complicated coupling of thermal lag of solid fuel with the boundary layer adjustment to external perturbations in hybrid rocket combustion. They proposed a linearized theory based on the mathematical perturbation method in order to predict the initiation of low frequency pressure oscillations. The results showed a good

* Corresponding author. Tel.: +82 2 450 3533.

E-mail addresses: skypks@konkuk.ac.kr (K.-S. Park), cjlee@konkuk.ac.kr (C. Lee).

¹ Graduate student.

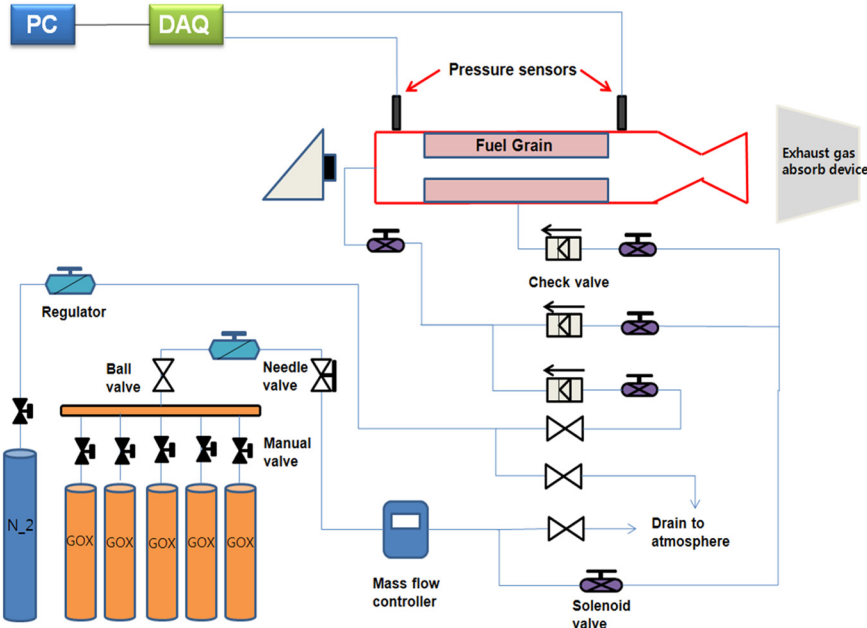


Fig. 1. Schematic of experimental set-up.

agreement with experimental data of pressure oscillations with a peak frequency up to 50 Hz.

Boardman et al. [1] observed sudden amplification of pressure oscillations during combustion processes. FFT analysis confirmed that the instability frequency lies in the range of less than 500 Hz. A peak frequency less than 50 Hz was dominantly identified in the spectral data. But, their study did not address the causes of combustion instability of low frequency. Korting et al. [6] also found that pressure oscillations were suddenly amplified during the combustion. Though the results did not include the spectral analysis of pressure oscillations, they suspected that the sudden increase in the regression rate was directly associated with the abrupt amplification of low frequency pressure oscillations.

Carmicino [2] performed a series of combustion tests with various injector configurations. The test results with radial type injectors showed combustion instability with a peak frequency of 10–30 Hz. They suspected the resonance of pressure perturbations due to unsteady heat releases in the post chamber and acoustic excitations of the main combustor as a triggering mechanism of combustion instability. They claimed that unsteady heat release was possibly related with periodic formation of large-scale vortex shedding into the post chamber producing additional pressure perturbations. However, their study did not account for the effect of flow modifications in the different chamber configurations such as chamber volume ratio, post chamber length, fuel port diameter, etc.

Meanwhile, Greiner and Frederick [3] conducted combustion tests to examine the effect of post chamber volume on the occurrence of instability in hybrid rocket combustion. They found that a sudden amplification of pressure oscillations occurred only at a certain value of volume ratio of main and post chambers. Unfortunately, no further reports were published addressing the correlation between the triggering mechanism of LFI and volume ratio.

Even though previous studies suggested the geometric chamber configuration can be a controlling parameter in determining the appearance of LFI, there are no comprehensive studies to bridge the gap between experimental observations and physical understandings on the triggering mechanisms of LFI. In this study, a series of experimental tests was designed to investigate the triggering mechanism of LFI, which was suddenly amplified at a certain

condition during the combustion. To this end, a couple of controlling parameters was selected and the sensitivity of each parameter to instability was evaluated, including volume ratios of main and post chambers, oxidizer mass flow rates, and solid fuel types. Also this study was focused on the modification in flow dynamic behaviors over the backward facing step in the post chamber by locating diaphragms at the rear end of fuel. In addition, the effect of time variation of fuel diameters on the initiation of instability was investigated.

2. Design of combustion tests

Fig. 1 shows the schematics of the experimental-setup. A series of hybrid rocket combustion tests was conducted with a laboratory-scale motor of GOx and PMMA combinations as an oxidizer and solid fuel, respectively. An axial type injector was used in all tests. Solenoid and check valves were used to control oxidizer feeding. The maximum capacity of mass flow controller was up to 40 g/s in the tests. Nitrogen gas was used to purge after the combustion by the PLC (Programmable Logic Controller) control. Piezo-type sensors were installed to measure the combustion pressure. DAQ board and Labview program were also implemented for data acquisition process. Dimensions of the baseline fuel have 50 mm and 20 mm of outer and inner diameters, respectively. In the baseline configuration, the chamber length of main, pre and post chambers were fixed as 200 mm, 45 mm and 75 mm, respectively. A water-cooled nozzle was used, in which a throat diameter and nozzle length were 6.5 mm and 40 mm, respectively.

Table 1 reports a summary of results of all test cases. A baseline test was made as a reference case, in which combustion pressure showed stable behavior and no distinctive LFI was found. Each test case has different configurations of main and post chamber length, whereas pre chamber length was kept unchanged. Here VR is the volume ratio between main and post chambers. The mass flow controller was used to control oxidizer mass flow from 10 g/s to 25 g/s for providing various O/F conditions. The average O/F ratio was calculated by dividing total oxidizer mass by regressed fuel mass during the test ($O/F = \int \dot{m}_{ox} dt / \Delta m_f$).

Tests 1 and 2 were designed to investigate the effect of post chamber length on the initiation of LFI. Test 3 was the case where the main chamber length increased as twice as that of baseline.

Table 1

Summary of combustion test results.

Test No.	Solid fuel	Chamber length (mm)	Post chamber length (mm)	Oxidizer mass flow rate (g/s)	O/F ratio	LFI	Remarks
Baseline	PMMA	200	75	20	5.20	No	Reference
1	PMMA	200	105	20	5.57	No	Volume ratio between main and post chamber
2	PMMA	200	200	20	5.59	No	
3	PMMA	400	75	20	2.35	Yes	
4	PMMA	400	105	20	2.41	No	
5	PMMA	400	200	20	2.46	No	
6	PMMA	400	75	10	2.23	Yes	Oxidizer mass flow rate
7	PMMA	400	75	15	2.29	Yes	
8	PMMA	400	75	25	2.43	Yes	
9	PMMA	400	75	20	2.31	Yes	Rear diaphragm
10	PMMA	400	75	20	2.28	Yes	Vortex shedding over a backward facing step
11	PMMA	400	75	20	2.23	Yes	Cutting rear edge
12	PMMA	400	75	20	2.32	Yes	
13 ^a	PMMA	400	75	20	2.43	Yes	Pressure sensitive combustion regime
14	HTPB	200	75	20	3.78	No	Fuel type
15	HTPB	200	40	20	3.60	Yes	

^a Nozzle throat diameter: 5.5 mm.

Tests 4 and 5 were designed to examine the effect of post chamber length in Test 3. Tests 6–8 were designed to investigate the effect of variation of oxidizer mass flow rate on the amplification of pressure oscillations. Tests 9–12 were performed to examine how the formation of vortex shedding over backward facing steps can affect the initiation of LFI. Test 13 was done with a reduced throat diameter from 6.5 mm of baseline case to 5.5 mm to increase a chamber pressure level. The fuel regression rate is mainly governed by diffusional heat flux in the turbulent boundary layer. However, with reduced combustion pressure, the regression rate becomes pressure sensitive. In this regard, Test 13 was designed to investigate the effect of combustion pressure on the onset of instability. Finally, Tests 14–15 were carried out to investigate the responses of combustion pressure in a different solid fuel of HTPB substituted with PMMA. One of interesting results was a correlation between volume ratio (VR) and LFI. The results showed that the test cases only with a volume ratio of 0.80–0.85 (Test cases 3 and 15) showed LFI. Further studies will be necessary to understand physical relations between volume ratio and the initiation of LFI.

Fig. 2 shows the comparison of geometrical configurations in Tests 2 and 3. Here, D_p represents an inner diameter of solid fuel. LFI was observed in Test 3 while Test 2 did not show any unstable combustion behaviors. The result confirmed that the low frequency characteristics of combustion pressure are quite dependent upon the geometrical configuration, including the length and the volume of main and post chambers. Further details will be described in the following sections.

3. Baseline results

The baseline test was carried out with PMMA and GOx at a constant oxidizer flow rate of 20 g/s to collect reference test data. Physical dimensions were briefly summarized in Table 1. The main chamber had a length of 200 mm and the post chamber length was set to be 75 mm. Fig. 3 shows a combustion pressure curve in baseline test. It displays a stable pressure trajectory of about 105 psi (7.24 bar) with moderate amplitudes of approximately 5 psi (0.34 bar). The oxidizer supply pressure was successfully controlled at about 180 psi (12.41 bar) to maintain the constant oxidizer flow rate of 20 g/s.

Fig. 4 is the FFT (Fast Fourier Transform) analysis of combustion pressure oscillations of baseline tests in the spectral domain of 0–800 Hz. Here the amplitude in Fig. 4 is the power spectral den-

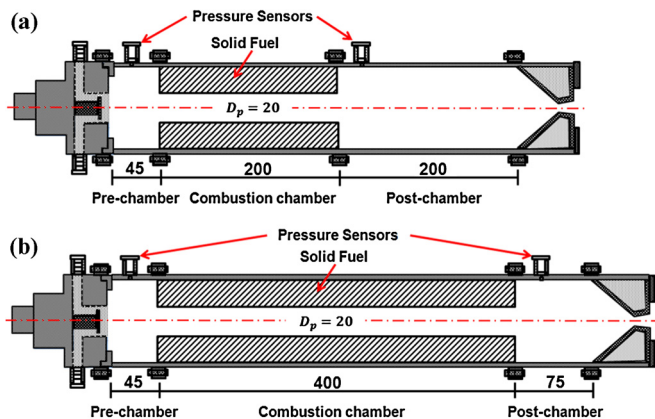


Fig. 2. Schematic of test configurations for a) Test 2, b) Test 3.

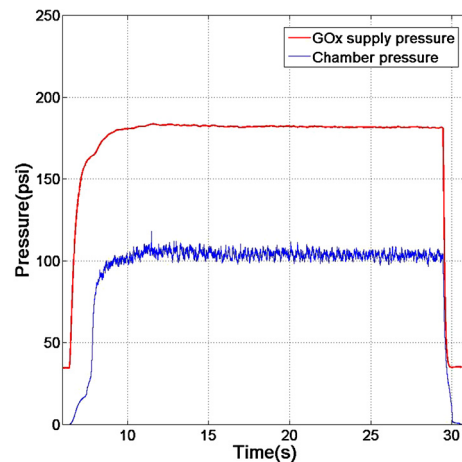


Fig. 3. Trajectory of combustion pressure of baseline.

sity of pressure oscillations in the spectral domain. Spectral data showed that the dominant frequencies of combustion pressure lie in the range of about 10–15 Hz, which approximately coincides with the frequency range responsible for thermal lag oscillations frequently observed in the combustion of solid propellants [5]. Other frequency bands were also identified in the spectral domain with the frequency range of 450–550 Hz, 500–600 Hz and

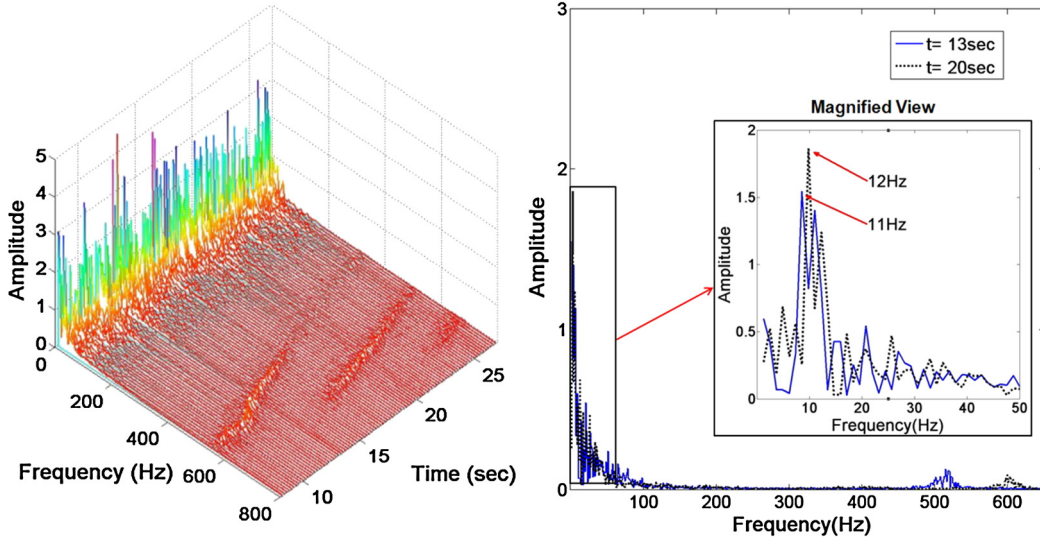


Fig. 4. Frequency waterfall and peak frequency for baseline.

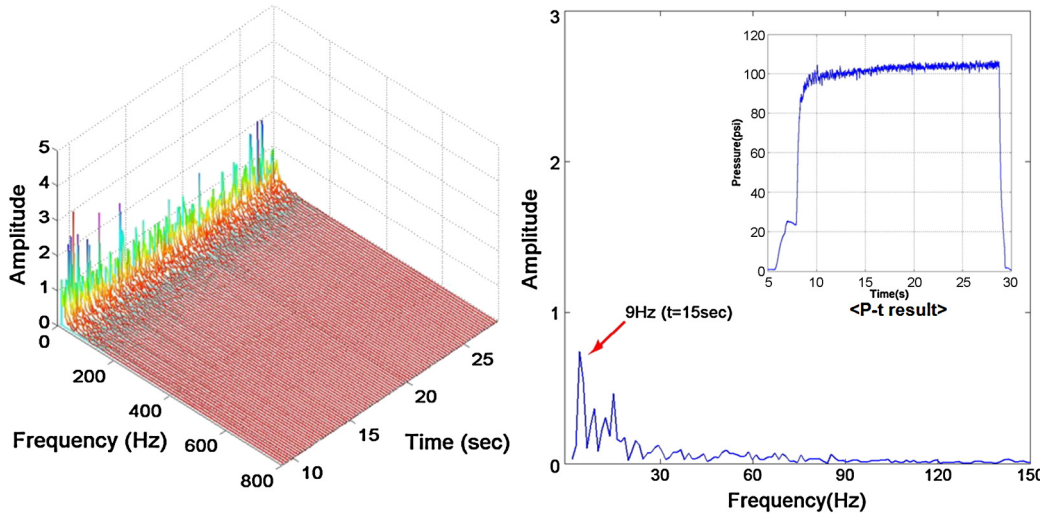


Fig. 5. Frequency waterfall and peak frequency for Test 2.

600–650 Hz, respectively, though the amplitudes were negligibly small compared to those of low frequency oscillations. Details of each frequency range and the initiation mechanism are described in the literature [8].

4. Pressure curves and spectral data in Tests 2 and 3

Test 2 was designed to examine the combustion characteristics of pressure oscillations by only increasing the post chamber length from the baseline length of 75 mm to 200 mm. In this case, the combustion pressure was stably maintained at about 105 psi (7.24 bar). Fig. 5 is the spectral analysis of combustion pressure oscillations showing a frequency range of 9–20 Hz, which is qualitatively the same range as that of the baseline case. However, the disappearance of frequency peaks of above 100 Hz was observed. Since the increase in the post chamber length was able to provide more volume, small-amplitude oscillations with a frequency above 100 Hz were easily damped out in a larger volume.

Test 3 was attempted to investigate the effect of changes in the combustion chamber volume on the initiation of LFI by increasing the main chamber length from 200 mm to 400 mm while the post chamber length was kept unchanged at 75 mm as in the baseline. Note that VR in this case was 0.85. Fig. 6 shows the trajectory

of combustion pressure in Test 3. The magnitude of peak-to-peak amplitudes suddenly increased from stable level up to around 30 psi (2.07 bar) at the moment of 14 s of combustion and lasted about three seconds. Spectral analysis showed that pressure oscillations with a peak frequency of 17 Hz were dominantly active in the amplifications. After the end of the first amplification, the second amplification with 14 Hz appeared in a row at the time of 23 s as well. The amplitudes of the second amplification were less than those measured at the first one. In literature, combustion instability was defined as a case where the amplitude of pressure oscillations exceeds 5% of an average pressure. According to this criterion, oscillations in Test 3 with amplitudes larger than 23% and 15% of mean pressure can be classified as the exhibition of LFI.

Note that the oxidizer flow rate in Test 3 was controlled to maintain at 20 g/s. However, pressure measurements showed that the oxidizer supply pressure slightly increased from the mean pressure of 210 psi (14.48 bar) at the moment of LFI, because the onset of combustion instability affected to increase the supply pressure in the upstream of injectors through the flow controller. A magnified view of pressure curve in Fig. 6 clearly showed that the first amplification was independent of an increase in the oxidizer supply pressure.

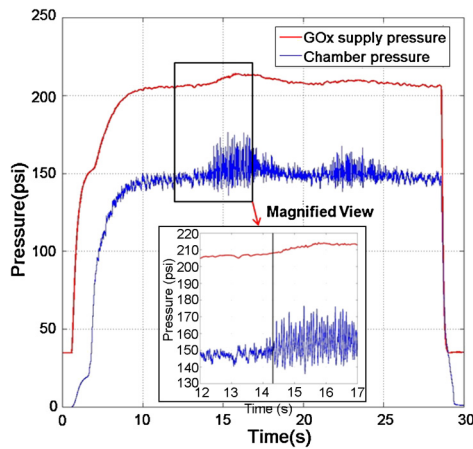


Fig. 6. Trajectory of combustion pressure and oxidizer supply pressure in Test 3.

Fig. 7 shows the frequency waterfall and peak frequencies of pressure curves in Test 3. Pressure oscillations suddenly amplified up to three times larger magnitudes than those in the baseline case. In this case, even though the peak frequency of instability was shifted toward a higher one of 14–17 Hz compared to the baseline, LFI in Test 3 seems to be the result of resonating two different oscillation mechanisms: pressure oscillations already existed in the baseline test and the unknown source of oscillations in the combustion. In this regard, Karabeyoglu et al. claimed that LFI is the result of complex coupling of thermal transients in solid fuels, known as thermal lags, and the transitional adjustment of the turbulent boundary layer to external perturbations [5].

In general, a thermal lag in the solid fuel is known as the source of typical oscillations with a frequency of 10–30 Hz determined by a solid fuel type and combustion conditions. Thus, the current study focuses on understanding the initiation processes of sudden amplification of pressure oscillations using the resonance of thermal lag and the unknown source of pressure perturbations caused by the change in the chamber configuration. In addition, oxidizer flow rates and fuel types were also selected as control parameters to assess their sensitivity to LFI initiation.

4.1. Controlling oxidizer mass flow rate and solid fuel

Tests 6–8 were designed to investigate the effect of controlling the oxidizer mass flow rate on the initiation of LFI. In the tests, the oxidizer flow rate was controlled to provide different O/F con-

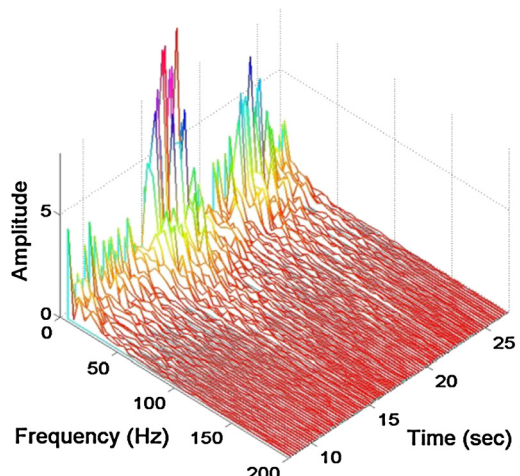


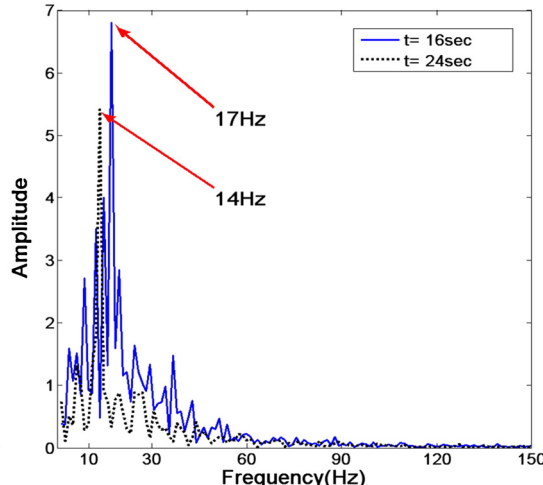
Fig. 7. Frequency waterfall and peak frequency of oscillation in Test 3.

ditions while other parameters were kept unchanged as used in Test 3. All tests were done to modify flow characteristics in the fuel grain with different mass flow rates. Test time was set to 22 s for all test cases.

Fig. 8 depicts a summary of pressure curves with different oxidizer mass flow rates and the variation of O/F ratio in Tests 3, 6, 7 and 8 by increasing the oxidizer flow from 10 g/s to 25 g/s in each test. The pressure oscillations were amplified in all cases at a certain moment of combustion. The first amplifications happened at 7, 8, 10 and 14 s of combustion depending on oxidizer flow rates in each test. As seen in **Fig. 8(a)**, the amplification appeared at an earlier time of combustion as the oxidizer flow rate increased. However, the second amplification of oscillations was not observed in Tests 6 and 7. Also, the variation of fuel diameters during combustion is displayed in **Fig. 8(b)** with two horizontal lines representing the fuel diameters at which pressure amplifications occurred respectively. Note that the regression rate in Test 3 was measured as approximately 0.25 mm/s, which showed a good agreement with the prediction of 0.27 mm/s from Ref. [10]. The time variations of fuel diameter in Tests 3 and 6–8 were displayed altogether in **Fig. 8(b)** based on the predictions of fuel regression rates in Ref. [3]. Critical fuel diameters corresponding to pressure amplification in each test were calculated by the time variation of fuel diameters in **Fig. 8(b)**. And the calculation confirmed that the critical fuel diameters in Tests 6–8 were found approximately 24 and 28 mm respectively. Note that the final fuel diameter in Tests 6 and 7 did not reach a critical diameter at which the second amplification occurred. This can explain the reason why the second oscillation was not observed in Tests 6 and 7. Even though the detailed mechanism of consecutive appearance of instability was not fully understood yet, the results showed that the initiation of LFI was not directly associated with the variation of oxidizer mass flow rates but with the variation of fuel diameters.

Next, Tests 14–15 were carried out with different solid fuels by substituting PMMA with HTPB to explore the effect of solid fuels on the initiation of instability. **Fig. 9** shows a combustion pressure trajectory in Test 15 with HTPB. The pressure oscillations were amplified immediately after the ignition developing into LFI more quickly than Test 3 with PMMA. The lower density and easy evaporating properties of HTPB are responsible for the earlier appearance of LFI than in PMMA. Generally, HTPB regressed very quickly than PMMA approaching its critical diameter where instability can be initiated.

Fig. 10 exhibits a frequency waterfall and peak frequency of combustion pressure oscillations in Test 15. The peak frequency in Test 15 was slightly shifted to higher one of about 20–30 Hz



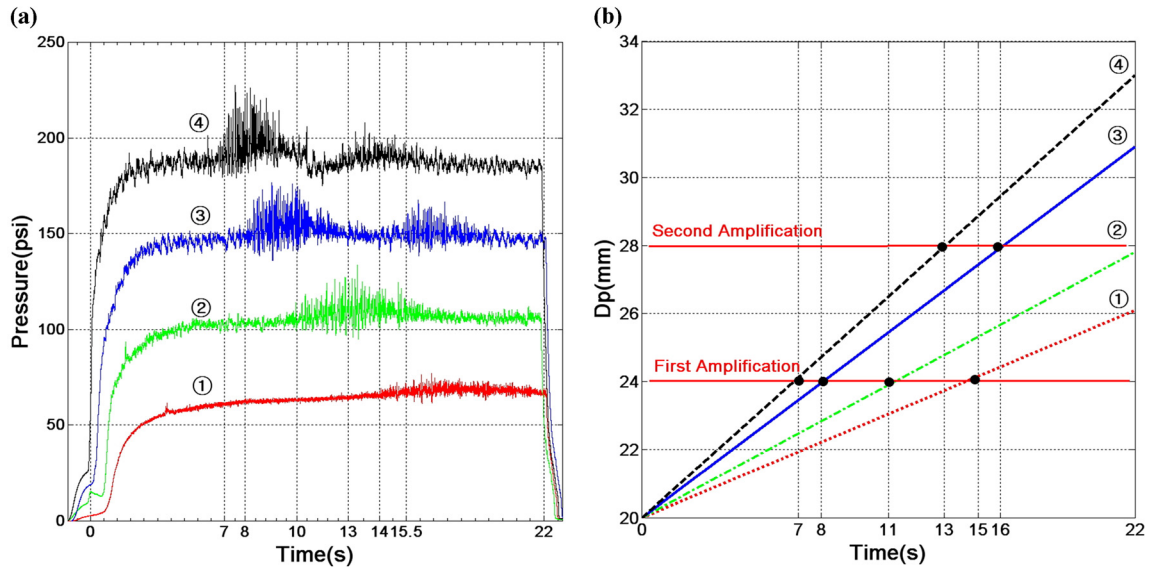


Fig. 8. P-t results and the variation of port diameter with different oxidizer flow rate ① Test 6, ② Test 7, ③ Test 3, ④ Test 8.

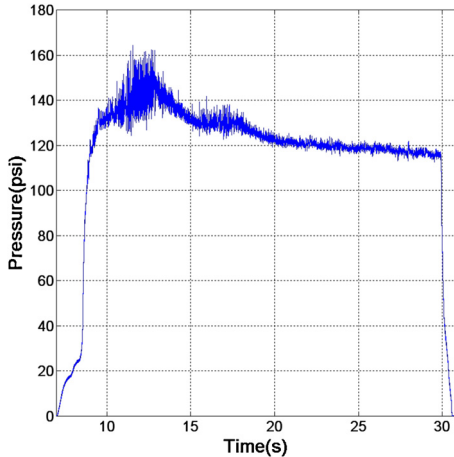


Fig. 9. Trajectory of combustion pressure in Test 15 with HTPB.

than those in Test 3 with PMMA. Note that the dominant frequency of oscillations in stable combustion was mainly determined by the thermal property of solid fuel HTPB due to thermal lags. The estimation of peak frequency of HTPB combustion was found

about 15–25 Hz [7,5]. Thus, the occurrence of LFI in Test 15 can be the result of resonating thermal lag oscillations of HTPB with the unknown source of pressure perturbations. Therefore, the results in Tests 3, 6–8 and 15 suggest that the occurrence of LFI would be independent of either the material property, fuel composition or oxidizer mass flow. The initiation of instability seemed to be closely associated with flow modifications induced by the change in chamber configuration including main and post chamber volume and length.

4.2. Fuel regression vs. LFI initiation

Reviewing the results of Tests 3 and 6–8, it was found that LFI initiated at a certain time of combustion or at a certain fuel diameter. In general, the inner diameter of solid fuels gradually increased as combustion proceeded. Test 8 was repeatedly done to measure the critical fuel diameter by stopping oxidizer supply at which LFI initiated. Fig. 11 shows the entire pressure curve recorded in Test 8 and a part of pressure curve terminated at the instant of LFI. Critical diameters corresponding to the first and second amplification in Test 8 were averaged with several measurements and found to be about 24 and 28 mm, respectively. As mentioned in the previous section, the critical diameter corresponding to the first ampli-

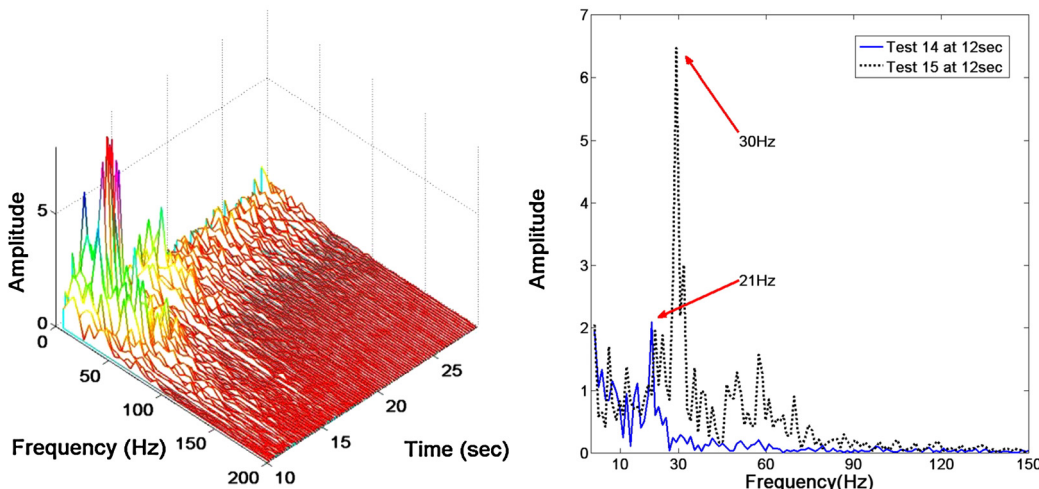


Fig. 10. FFT waterfall and peak frequency in Test 15.

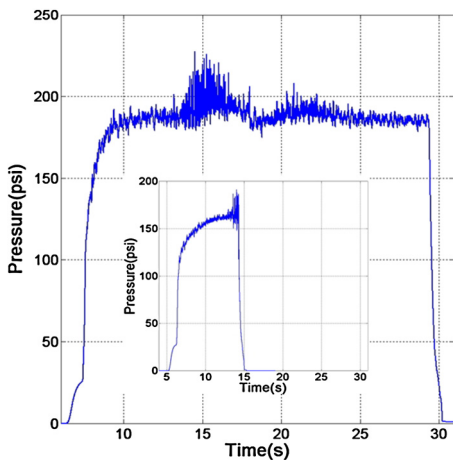


Fig. 11. Trajectory of combustion pressure in Test 8.

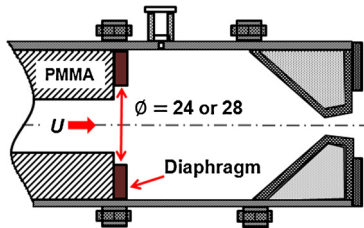


Fig. 12. Schematic of post chamber equipped with rear diaphragm.

fication in Tests of 3, 6 and 7 was also calculated about 24 mm from Fig. 8. This result suggests that the time variation of fuel diameter takes a very important role in determining the occurrence of LFI during the combustion through the unknown mechanism of perturbations. Since the difference in diameter between fuel grain and post chamber is step height, the time variation of fuel diameters brought into a continuous reduction in step height and consequently weakened vortex strength in the post chamber. If the initiation of LFI would be associated with the formation of vortex flow in the post chamber, the installation of diaphragm with a diameter of 24 mm could artificially produce pressure perturbations, which leads to LFI during the combustion. This is one of the possible scenarios that can explain the initiation of LFI in the combustion.

In order to assess the sensitivity of the time variation of fuel diameters to the initiation of LFI, Tests 9 and 10 were done with different rear diaphragms. Each diaphragm has the same inner di-

ameters of 24 and 28 mm as measured in Test 8. Fig. 12 shows a schematic diagram of post chamber configuration installed with rear diaphragms of diameters of 24 and 28 mm, respectively. Each test was done at the same test condition as used in Test 3.

Fig. 13 depicts a summary of pressure traces in each test with a rear diaphragm. The abrupt amplification of oscillations occurred at the instant where fuel diameters regressed toward the diaphragm diameter of 24 mm. Unlike the pressure curves in Test 3, LFI sustained to oscillate without any damping until the end of the test. In Test 10 with a rear diaphragm of $\phi = 28$ mm, the pressure amplification similarly occurred again even though the amplitudes were smaller than those in Fig. 13(a). Based on the test results with diaphragms, the initiation of LFI was directly related to the time variation of fuel inner diameters or somehow the change in combustion chamber volume due to the fuel regression.

Fig. 14 displays the frequency peaks of pressure curves in each test case (a) and (b) in Fig. 13. Peak frequencies in both cases lied in the same frequency range of 11–17 Hz as ones previously identified in Test 3.

4.3. Vortex shedding over backward facing step

Results in Tests 9 and 10 revealed that LFI suddenly occurred at certain fuel diameters during the combustion. Thus, it is natural to suspect the variation of geometrical shape of backward facing steps in the post chamber to be a critical parameter in triggering LFI. Since the height of a backward facing step is the diameter difference between post chamber and fuel port, the regression of solid fuels continuously reduced step height and also affected the inflow patterns of combustion gas into the post chamber including the strength of vortex shedding. To estimate the effect of vortex shedding on the initiation of LFI, additional tests were designed with solid fuels having different rear edge angles of 30 and 60 degrees. Test condition was maintained as the same one as used in Test 3. Fig. 15 shows the schematic diagram of rear edges with different cutting angles of 30 and 60 degrees, respectively.

Fig. 16 shows the trajectories of combustion pressure of tests with different cutting angles. For the 60-degrees edge angle, the overall pattern of pressure oscillations was very similar to the oscillations already observed in Test 3, showing two consecutive pressure amplifications. However, pressure curves with the 30-degrees cutting angle exhibited a relatively stable combustion without second amplification.

Fig. 17 displays the spectral analysis of peak frequency between two cases. The peak frequency in both cases was dominantly active in the range of 14–18 Hz, which is similar to one of 15–20 Hz as observed in Test 3.

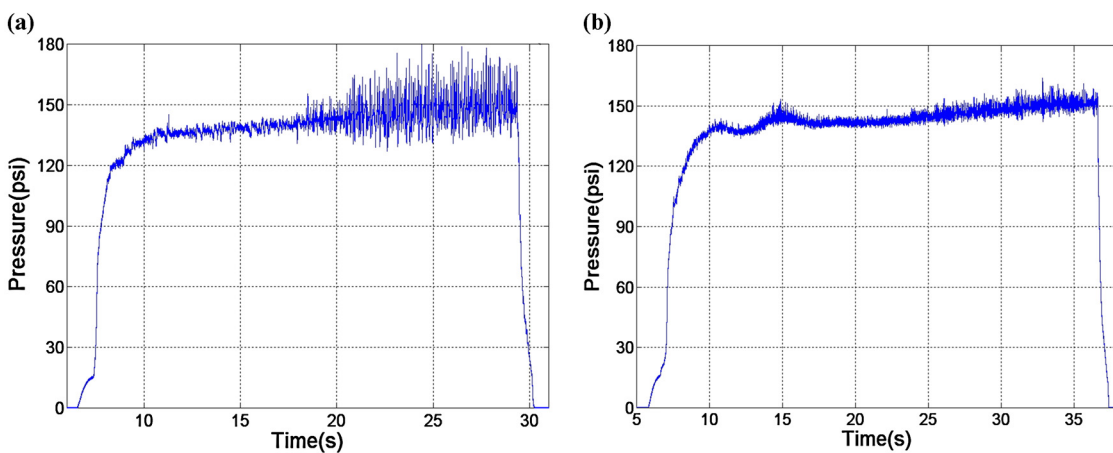


Fig. 13. Pressure trajectories with a rear diaphragm (a) Test 9 ($\phi = 24$ mm), (b) Test 10 ($\phi = 28$ mm).

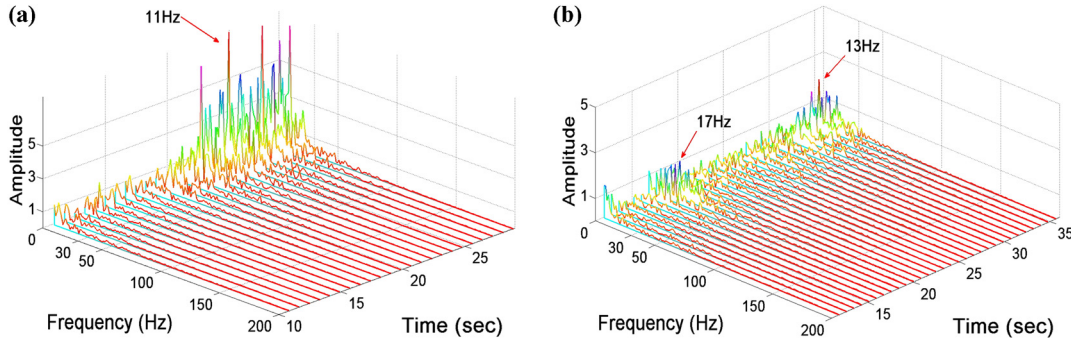


Fig. 14. Peak frequency in LFI with rear diaphragms (a) Test 9 ($\phi = 24$ mm), (b) Test 10 ($\phi = 28$ mm).

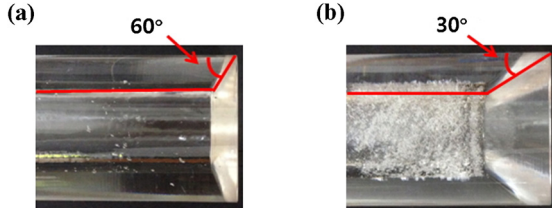


Fig. 15. Variation of edge cutting angle at rear end (a) Test 11 (60°), (b) Test 12 (30°).

In summary, the variation of edge cutting angles did not completely modify the occurrence of LFI even though the cutting rear edge of solid fuels contributed to slightly reduce the oscillation amplitudes. Therefore, the scenario that the vortex formation in the post chamber is critically responsible for the initiation of LFI has to be reviewed again. In this regard, a hypothesis can be suggested regarding the critical role of vortex shedding in the post chamber. If the vortex shedding consisted with unburned mixtures over a backward facing step would flow into the post chamber, it could generate unsteady heat releases and additional low frequency pressure perturbations as a result of continuing combustion in the post chamber as well. Pressure oscillations would be suddenly amplified, leading to LFI in the case of resonating with existing stable pressure oscillations by the thermal lag of solid fuels. Even though the test results in Fig. 13 partially confirmed the validity of the hypothesis of the initiation of LFI, the hypothesis is not suitably providing possible physical explanations on the persistent occurrence of LFI in the tests with different edge cutting angles shown in Fig. 16. A further study will be required to understand the correlation of the initiation of LFI in connection with

vortex shedding patterns or strength over a backward facing step in the post chamber.

4.4. Effect of combustion pressure

Wooldridge et al. [9] investigated that LFI could possibly occur if the combustion pressure was maintained below a critical pressure where the regression rate was dependent on the chamber pressure. In this combustion condition, fuel combustion was very sensitive to the change in combustion pressure. And the pressure perturbations could lead to the development of LFI. Therefore, Test 13 was additionally designed to understand if the pressure level of about 150 psi (10.34 bar) in Test 3 was in the pressure sensitive regime. To this end, the test was done with the increased chamber pressure of about 190 psi (13.10 bar) by reducing the nozzle throat diameter from 6.5 mm to 5.5 mm. Here, other test conditions were kept unchanged as used in Test 3.

Fig. 18 shows the trajectories of combustion pressure oscillations in Test 13. Pressure oscillations were amplified immediately after the ignition producing two consecutive occurrences of instability. The overall behavior of pressure oscillations was very similar to those in Test 3 in which two consecutive pressure peaks occurred.

Fig. 19 displays the spectral analysis of peak frequency of 14–16 Hz in Test 13, the similar range of peak frequency as observed in Test 3. If LFI in Test 3 would be initiated by the pressure sensitiveness of fuel regression, the increase in combustion pressure could shift combustion dynamics rather toward stable combustion because the fuel regression was not dependent on the combustion pressure anymore. However, the pressure trajectory in Test 13 is very similar to those in Test 3 in two ways. The first

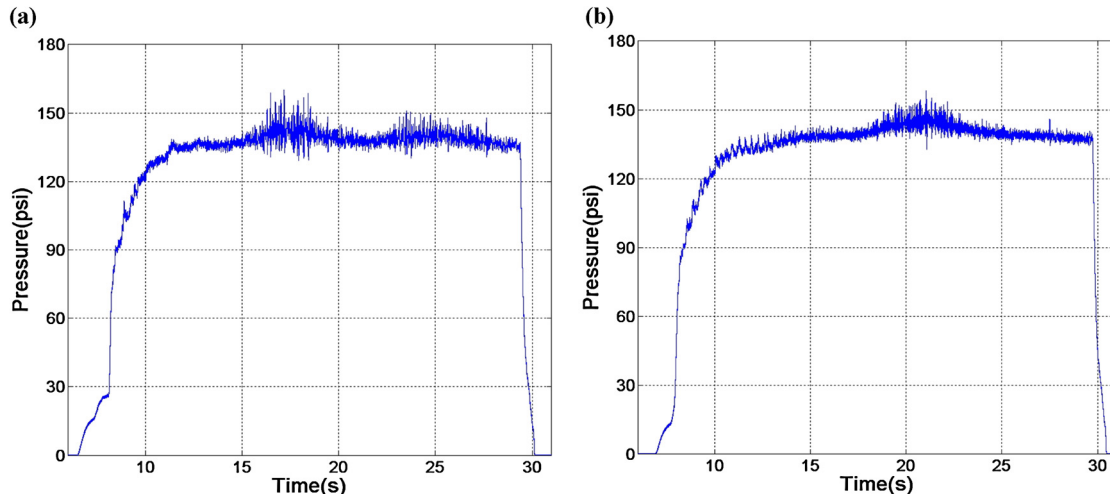


Fig. 16. P-t results with cutting of backward-step (a) Test 11 (60°), (b) Test 12 (30°).

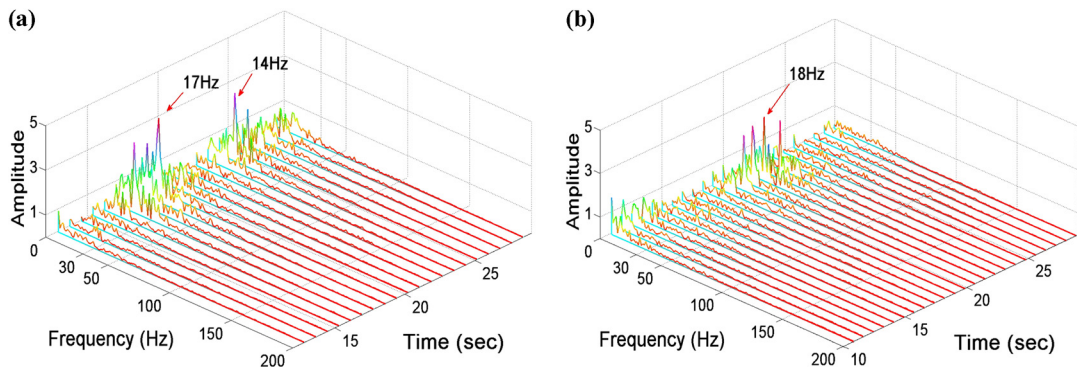


Fig. 17. Peak frequency results with cutting of backward-step (a) Test 11 (60°), (b) Test 12 (30°).

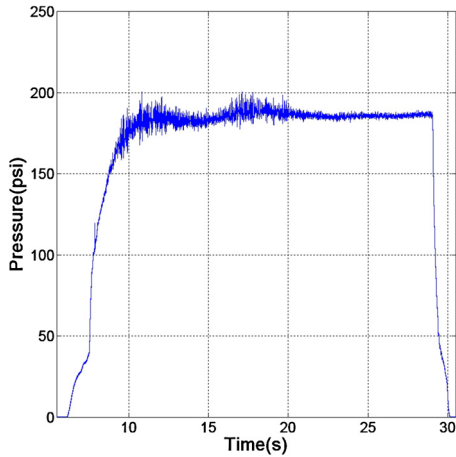


Fig. 18. Trajectory of combustion pressure in Test 13.

one is the persistent occurrence of LFI. And the other one is the consecutive appearance of two amplifications. Thus LFI in Test 3 was surely not the result of pressure coupling with fuel regression behaviors in the pressure sensitive combustion regime.

5. Conclusion

This study considered about the triggering mechanism of LFI that is frequently observed in laboratory-scale hybrid rocket mo-

tors. To this end, a series of experimental tests was designed and performed with selected parameters, including volume ratios between main and post chambers, oxidizer mass flow rates, fuel types and backward facing step configurations in the post chamber.

In the baseline test, combustion showed very stable pressure oscillations with the predominant peak frequency range of 10–15 Hz. However, pressure oscillations in Test 3 suddenly jumped into unstable mode, leading to LFI with a peak frequency of 14–17 Hz. Test 3 was done with the combustion chamber length increased from 200 mm to 400 mm. The dominant frequency of 14–17 Hz in Test 3 was interestingly the same frequency as those observed in the stable combustion of solid fuels due to thermal lags. Moreover, the experimental results in Tests 3, 6–8 and 15 suggested that the occurrence of LFI was insensitive to the change in the material property, the composition of solid fuels and the variation of oxidizer mass flows. Interestingly, LFI suddenly initiated at the moment where the fuel diameter regressed approaching to a certain diameter of 24 and 28 mm respectively. The initiation of instability was closely associated with the change in flow dynamics induced by the modification of combustion chamber configuration including main and post chamber volume and length.

In addition, the results with rear diaphragms confirmed that the time variation of height of backward facing step due to fuel regression significantly affected the instability characteristics by reducing peak amplitudes and changing initiation patterns, but it could not completely alter or control the occurrence of LFI. In this aspect, a hypothesis was introduced to examine a critical role of

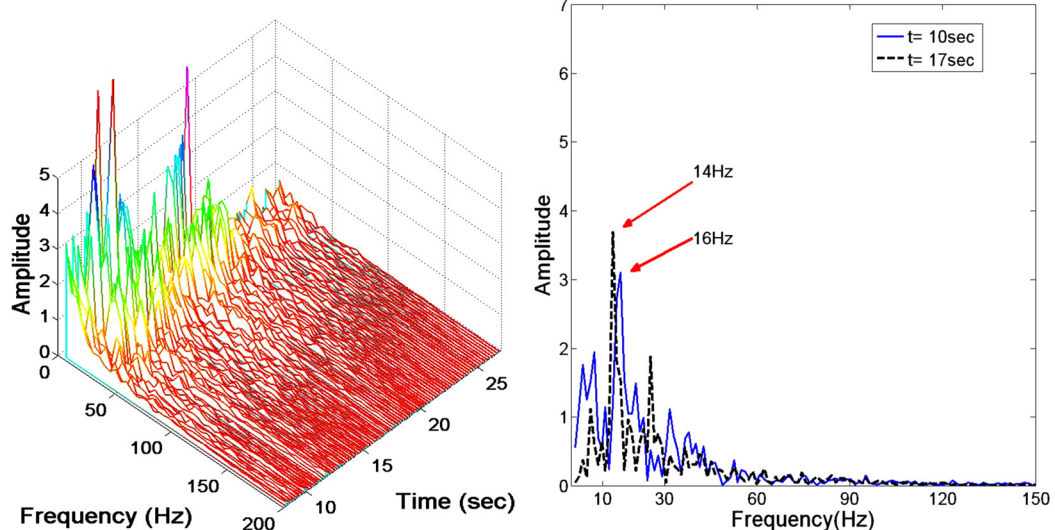


Fig. 19. FFT waterfall and peak frequency in Test 13.

vortex shedding in the post chamber. If the vortex shedding over backward facing step would flow into the post chamber with partially burned mixtures, it could generate unsteady heat releases as the result of continuing combustion and additional low frequency pressure perturbations in the post chamber as well. Pressure oscillations in the stable combustion by a thermal lag of solid fuels would be suddenly amplified, leading to LFI in the case of resonating with pressure oscillations associated with vortex shedding in the post chamber. Even though the test results in Fig. 13 partially confirmed the validity of the hypothesis, details of triggering mechanism remain still unveiled yet. Further study may focus on the vortex shedding and the generation of pressure perturbations in the post chamber using both experiments and numerical calculations.

Conflict of interest statement

I declare that I have no conflict of interest.

Acknowledgements

This work was supported by 2011 research fund of National Research Foundation of Korea (2011-0027980).

References

- [1] T.A. Boardman, R.L. Carpenter, S.E. Clafin, A comparative study of the effects of liquid-versus gaseous-oxygen injection on combustion stability in 11-inch-diameter hybrid rocket, in: 33th Joint Propulsion Conference and Exhibit, in: AIAA 97-2936, 1997.
- [2] C. Carmicino, Acoustic, vortex shedding, and low-frequency dynamics interaction in an unstable hybrid rocket, *J. Propuls. Power* 25 (6) (2009).
- [3] B. Greiner, R.A. Frederick, Results of labscale hybrid rocket motor investigation, in: 28th Joint Propulsion Conference and Exhibit, in: AIAA 02-3301, 1992.
- [4] R.M. Jenkins, J.R. Cook, A preliminary analysis of low frequency pressure oscillations in hybrid rocket motors, in: 31th Joint Propulsion Conference and Exhibit, in: AIAA 95-2690, 1995.
- [5] A. Karabeyoglu, S. De Zilwa, C. Cantwell, G. Zilliac, Modeling of hybrid rocket low frequency instabilities, *J. Propuls. Power* 21 (2005) 1107–1116.
- [6] P.A.O.G. Korting, H.F.R Shoyer, C.W.M. Van der Geld, On the use of an ultrasonic pulse-echo technique for regression rate analysis, SFCC-publication, No. 24, 1987.
- [7] C. Lee, The application of ZN analysis to the transient combustion of hybrid rocket, in: 40th AIAA Aerospace Sciences Meeting & Exhibit, in: AIAA 2002-0783, 2002.
- [8] K. Park, K. Shin, C. Lee, Vortex shedding and pressure oscillations in hybrid rocket, *J. Korean Soc. Aeronaut. Space Sci.* 41 (1) (2013) 40–47.
- [9] C.E. Wooldridge, G.A. Marxman, R.J. Kier, Investigation of combustion instability in hybrid rocket, NASA CR-66812, 1969.
- [10] G. Zilliac, A. Karabeyoglu, Hybrid rocket fuel regression rate data and modeling, in: 42th Joint Propulsion Conference and Exhibit, in: AIAA 2006-4504, 2006.